Deformation behaviour of cracked expansive soil subgrades under varied climatic conditions

Murugesan SankaraNarayanan*,[1], and Sathiyamoorthy Rajesh[2]

[1]*Research Scholar, Dept. of Civil Engineering, Indian Institute of Technology Kanpur, Kanpur 208016, India.* [2]*Professor, Dept. of Civil Engineering, Indian Institute of Technology Kanpur, Kanpur 208016.*

**Corresponding author's email:* sankaran20@iitk.ac.in

Abstract: Subgrade soils with high swelling tendency, such as expansive soil, pose significant risks to low-volume pavements. The fluctuation of moisture levels due to rainfall and subsequent evaporation causes significant volumetric changes in such soils, resulting in heave and settlement of the overlying pavement. Furthermore, desiccation cracks form as a result of pore water evaporation. Hence, estimating the deformation induced on pavements within the framework of unsaturated soil mechanics is crucial for its long-term durability. In this study, a finite element numerical model utilizing unsaturated dual-permeability theory is employed to analyze the deformation behaviour of low-volume flexible pavements supported by expansive subgrade soil. The unsaturated soil parameters, including the soil-water retention curve (SWRC), suction stress curve (SSC), and hydraulic conductivity function (HCF), were experimentally determined and integrated into the model. The study focuses on the influence of preferential flow induced by desiccation cracks on the heave and settlement characteristics of the subgrade soil, which are examined through detailed numerical simulations. The results indicate a notable variation in the pore water pressure profile of the subgrade when desiccation cracks are considered, leading to heave and settlement during both rainfall and dry seasons.

Introduction

Large deposits of swelling clay soils or expansive soils are found in Regina (Canada), close to one-fourth of the land in United States, nearly 20% of the land area in India, approximately 150 million acres in China, throughout western Australia, and in several other African and European countries. Such soils are often classified by civil engineers as problematic due to their tendency to undergo volume changes in response to seasonal moisture fluctuations. These changes, driven by water absorption during rainfall and moisture loss through evaporation, result in repeated swelling and shrinkage cycles. These deformations can induce stress as high as 1500 kPa, which is sufficient to cause significant permanent damage to the overlying light loaded structures including low-volume pavements [1]. FHWA NHI-05-037 (2006) [2] outlines that moisture fluctuations in the subgrade can lead to several types of distress in flexible pavements, including heave, differential settlement, rutting, roughness, distortion, and cracking. Additionally, high saturation levels in subgrade for prolonged period may reduce the subgrade

modulus by up to 50%, thereby shortening the operational life of the pavement [3]. Despite the development of techniques and extensive research to minimize these distresses, significant financial resources continue to be spent each year for the repair and maintenance of flexible pavements built on expansive soil subgrades [4]. This is because most of these researches are focussed on preventing moisture infiltration into the subgrade in heavy rainfall periods and ignore the drastic damages caused due to evaporation. With global warming becoming a huge problem, it is predicted that there will be prolonged periods of high temperatures in the coming years.

As previously mentioned, subgrade shrinkage resulting from moisture loss leads to the formation of cracks, commonly known as desiccation cracks. Following repeated swell-shrink cycles, a stable crack network forms, creating pathways that allow for the rapid infiltration of rainwater into the subgrade. This process, often referred to as preferential flow, accelerates the movement of water, air, and other fluids. Fig. 1 presents a schematic representation of water flux occurring within the pavement.

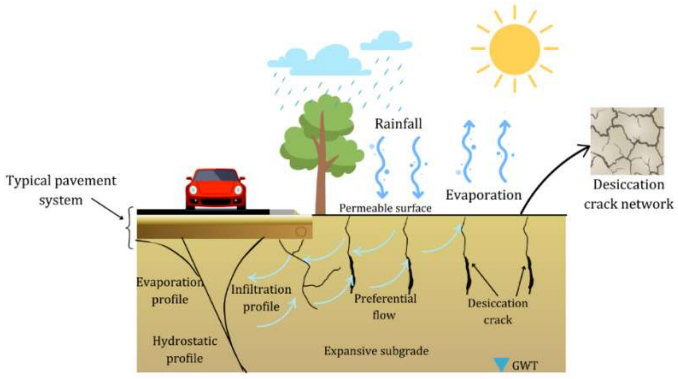

Figure 1: Schematic representation of water flux in a cracked expansive subgrade soil

This study applies the concept of unsaturated dual-permeability modelling to a finite element numerical model to predict the deformation behaviour of low-volume flexible pavements resting on expansive subgrade soil. The unsaturated parameters of the expansive soil - soil-water retention curve (SWRC), suction stress curve (SSC), and hydraulic conductivity function (HCF) were determined experimentally and incorporated into the numerical model. The study investigates in detail the impact of preferential flow through desiccation cracks on the heave-settlement behaviour of the subgrade soil through numerical analysis. A detailed description of the methodology, experimental study, and numerical modelling is provided in the following sections.

Unsaturated dual-permeability model

Unsaturated dual-permeability approach offers an effective modelling structure to analyze the flow through fractured medium. In this method, the pore structure in the cracked soil is treated as two distinct, yet interacting domains: micropores (soil aggregate pores) that represent flow

through the intrinsic voids; and macropores (cracks) that facilitate preferential flow through a much higher hydraulic conductivity than the micropores. This method provides a significant improvement over the traditional single-domain models, by using distinct Richard's equation for the dual-domains and incorporating an inter-domain transfer function, that allows simultaneous flow and moisture transfer between the domains. In the recent years, this method is widely used to model flow through fractured soils and rocks by several researchers ([5], [6], and [7]).

Gerke and Van Genutchen (1993) [8] provided the coupled Richard's equation between the macrodomain (denoted by subscript 'M') and microdomain (denoted by subscript 'm') to solve the flow in an unsaturated dual-permeability medium. Van Genutchen (1980) [9] model is used to describe the key unsaturated soil parameters: Soil Water Retention Curve (SWRC) and the relative hydraulic conductivity as follows,

$$S_e = \frac{\theta - \theta_r}{\theta_s - \theta_r} = [(1 + (|\alpha h|))^n]^{-m} \tag{1}$$

$$K = K_s K_r = K_s S_e^{0.5} [1 - \left(1 - S_e^{\frac{1}{m}}\right)^m]^2 \tag{2}$$

where θ, θ_s, θ_r are the volumetric water content, saturated volumetric water content and residual volumetric water content, S_e is the effective saturation, α (1/m), n, m are fitting parameters, K_s [m/s] is the saturated hydraulic conductivity and K_r is the relative hydraulic conductivity.

Coupled shrinkage and desiccation crack model

The model formulated by Stewart et al. (2016a) [10] is employed in the present study. The total porosity of the soil at any water content is the combination of a) desiccation crack porosity φ_{dc}, b) settlement porosity φ_{set} and c) matrix porosity φ_{matrix}, where φ_{dc} and φ_{set} correspond to macropores porosity φ_M, and φ_{matrix} correspond to micropores porosity φ_m. This model is based on the presumption that the crack network has attained a stable state after several wet-dry cycles.

A set of equations that relate SSC parameters and effective saturation to the porosity of each domain was given by Stewart et al. (2016a) [10] as follows:

$$\begin{aligned}
\varphi_m(S_e) &= (\varphi_{max} - \varphi_{min})\left(\frac{p+1}{p + S_{e,m}^{-q}}\right) + \varphi_{min} \\
\varphi_{set}(S_e) &= \left(1 - \left(1 - (\varphi_{max} - \varphi_{min})\right)^{r_s}\right)\left(\frac{1 - S_{e,m}^q}{1 + pS_{e,m}^q}\right) \\
\varphi_{dc}(S_e) &= \left((\varphi_{max} - \varphi_{min}) - 1 + \left(1 - (\varphi_{max} - \varphi_{min})\right)^{r_s}\right)\left(\frac{1 - S_{e,m}^q}{1 + pS_{e,m}^q}\right)
\end{aligned} \tag{3}$$

where φ_{max} is the micropore porosity corresponding to full saturated state and φ_{min} is the micropore porosity corresponding to complete dried state, r_s is the volume change parameter, and p, q are the fitting parameters of SSC.

The influence of swell-shrink behaviour of the multi-pore system on the hydraulic conductivity of the soil is described using a transient HCF for each domain [11] as follows:

$$K_M = K_{dc,max}\left(\frac{1 - S_{e,m}^{q}}{1 + pS_{e,m}^{q}}\right)^2 K_{r,dc}$$
$$K_m = K_{m,max}\left(\frac{p+1}{p + S_{e,m}^{-q}}\right)K_{r,m} \quad (4)$$

where $K_{dc,max}$ is the saturated hydraulic conductivity of desiccation crack at φ_{min}, $K_{m,max}$ is the saturated hydraulic conductivity of micropore at φ_{max} , $K_{r,dc}$ is the relative hydraulic conductivity of desiccation crack (taken as 1) and $K_{r,m}$ is the relative hydraulic conductivity of micropore (given by Eq. 2).

Heave and settlement prediction

According to the model discussed in the previous section, the vertical shrinkage due to the uniform settlement of the individual soil blocks leads to a single pore domain of porosity φ_{set}. The shrinkage in vertical direction (ΔH) is proportional to the total volumetric strain ($\Delta V/V$) through a volume change parameter, r_s which is equal to 3 for an isotropic shrinkage [12,13]. Hence, the vertical deformation of a soil of n layers (ΔH) at any water content from an initial state can be described as,

$$\Delta H = \sum_{i=1}^{n}\left(H_i\left(\varphi_{set,i}\left(S_{e,m}\right) - \varphi_{set,f}\left(S_{e,m}\right)\right)\right) \quad (5)$$

where H_i is the height of the i^{th} soil layer, $\varphi_{set,i}$ is the initial settlement porosity and $\varphi_{set,f}$ is the final settlement porosity.

Experimental Study

The highly swelling natural expansive soil used in the present numerical study was collected from a depth of 1 meter below the surface level in Trichy, India. From the preliminary laboratory investigation, the soil is classified as CH soil with a liquid limit of 57.2% and plastic limit of 20.43%. The free swell index of the soil was determined to be 280% (IS 2720-40 [14]), indicating that its expansive index is very high. The hydraulic characteristics of the expansive soil were determined on statically compacted specimens prepared at a dry density (1.65 g/cc) corresponding to OMC-2% (16.5%). Two measurement techniques were used to determine the drying SWRC data across low and high suction ranges. The axis translation technique, employed

for the low suction range (50-400 kPa), was carried out using a GDS unsaturated triaxial setup. For the high suction range (10^3-10^6 kPa), the dew-point potentiometer technique was used with a WP4C potentiometer. Detailed descriptions of specimen preparation and testing procedures for both methods can be found in Roy and Rajesh (2018) [15] and Jadar and Rajesh (2024) [16]. The experimental data were fitted to the Van Genuchten (1980) model, as shown in Eq. 1. Given the highly expansive nature of the soil, it is important to note that the specimens underwent volume changes during drying, which altered their initial state while measuring the SWRC. This volume change behaviour upon drying (SSC) was determined through a separate set of experiments, following the procedure outlined in Jadar and Rajesh (2024) [16], and was fitted using Eq. 3. Fig. 2a and 2b shows the fitted SWRC and SSC curves with the experimental data points. By combining this with the fitted SWRC in the gravimetric water content-suction (w_g-Ψ) plane, the SWRC in the volumetric water content-suction (θ-Ψ) plane was derived.

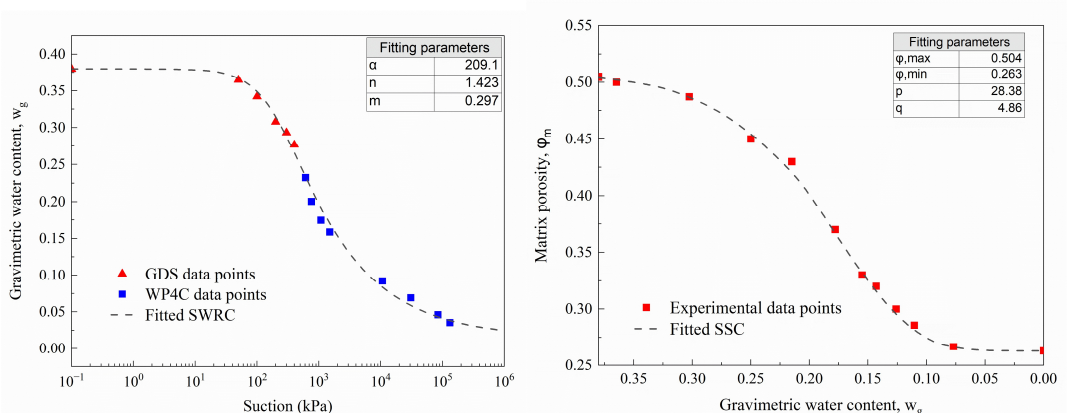

Figure 2: a) SWRC in gravimetric plane and b) SSC

Numerical modeling

The numerical analyses were performed in a commercial finite element program COMSOL Multiphysics (version 6.1). Since desiccation cracks predominantly occur within the surficial soil layers, the influence of overburden stress is considered insignificant. Consequently, the numerical analyses disregard the effects of mechanical stress and is formulated as a purely hydraulic model. Here, the pavement layers are not explicitly modelled since the scope of this study is on the expansive subgrade, which governs the heave and settlement due to moisture fluctuations. Since the effective drainage characteristics in the pavement system prevents direct moisture infiltration, the pavement surface is considered to be impermeable in the numerical model. In this study, a 5 m-wide section of a low-volume flexible pavement lane constructed over a 5 m layer of expansive soil from the Trichy region is numerically modelled. The surficial layer of 2 m is considered to develop desiccation cracks during drying and is modelled using the dual-permeability framework. Additionally, to evaluate the influence of desiccation cracks on pavement heave and settlement, a comparative model without a cracked layer is also analyzed.

The initial groundwater table (GWT) is set at the base of the model. To replicate field conditions, the initial pore water pressure distribution is established by applying an evaporation rate of 5 × 10^{-9} m/s over a one-year period. The flux boundary condition at the permeable surface incorporates recorded rainfall (Fig. 3) and actual evaporation data for the Trichy region over a 365-day period from January 1, 2023, to December 31, 2023. Fig. 4a shows the schematic details of the finite element model with all the boundary conditions and Fig. 4b shows the final meshed numerical model. The model parameters for both the matrix domain are derived from experimental investigations, as summarized in Table 1.

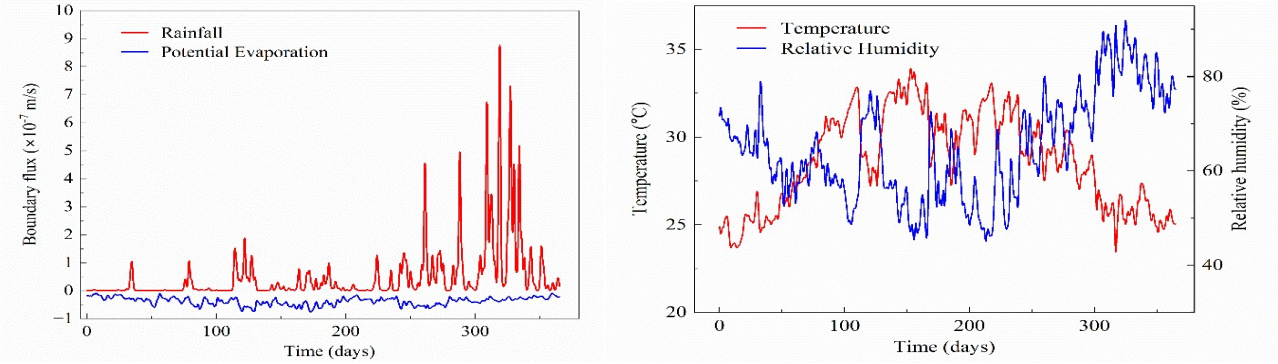

Figure 3: a) Input rainfall and potential evaporation data and b) Temperature and relative humidity data

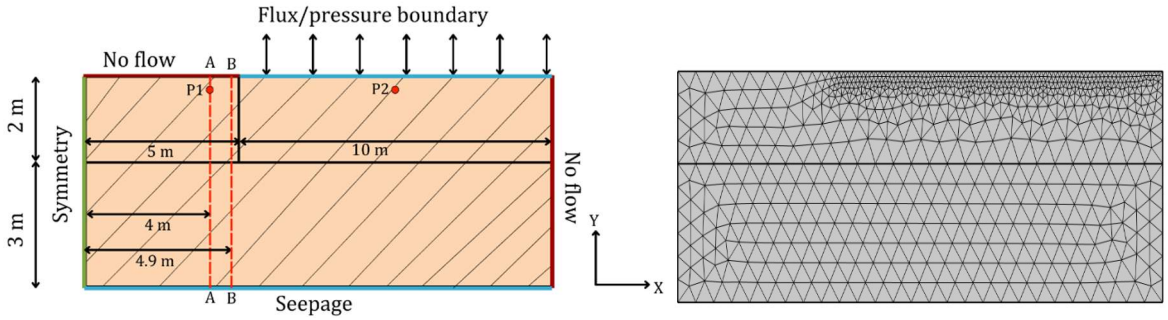

Figure 4: a) Schematic representation of numerical model and b) Meshed finite element model

Results and discussion

Variation of crack volume

Fig. 5a illustrates the temporal variation of desiccation crack porosity (φ_{dc}) at two observatory points, P1 and P2. The rainfall pattern, depicted in Figure 5a, highlights two distinct seasonal periods: the dry season (0–241 days) with minimal rainfall and the wet season (241–334 days) characterized by heavy rainfall. During the dry season, φ_{dc} exhibits a notable increase, indicating the expansion of crack volume due to moisture loss.

The variation at P1 is almost same as that of P2, despite the absence of direct evaporation from the subgrade through the pavement surface. The increase in φ_{dc} at P1 can be attributed to the interconnected desiccation crack network, which provides a preferential pathway for moisture migration towards the permeable surface from the subgrade. Even though the initial porosity at P1 is relatively small, the interconnection of cracks facilitates significant moisture transport. In contrast, during the wet season, the cracks begin to close as rainfall infiltrates the soil, causing φ_{dc} to decrease. By the end of the wet season, φ_{dc} approaches zero, signifying the closure of cracks due to increased soil moisture content.

Table 1: Model parameters for the numerical model

Model Parameter	*Symbol (unit)*	*Crack domain*	*Matrix domain*
SWRC fitting parameters	α *(1/m)*	1.5	0.0433
	n *(-)*	2	1.423
	m *(-)*	0.5	0.297
	θ_s *(-)*	0.99	0.505
	θ_r *(-)*	0.01	0.056
SSC fitting parameters	p *(-)*	-	28.38
	q *(-)*	-	4.86
	φ_{max} *(-)*	-	0.504
	φ_{min} *(-)*	-	0.263
Saturated hydraulic conductivity (m/s)	$K_{m,max}$ *(m/s)*	20.44	8×10^{-9}
Interporosity flow coefficient	α_{ws} *(1/m²)*	10 (Luo et al. 2023)	

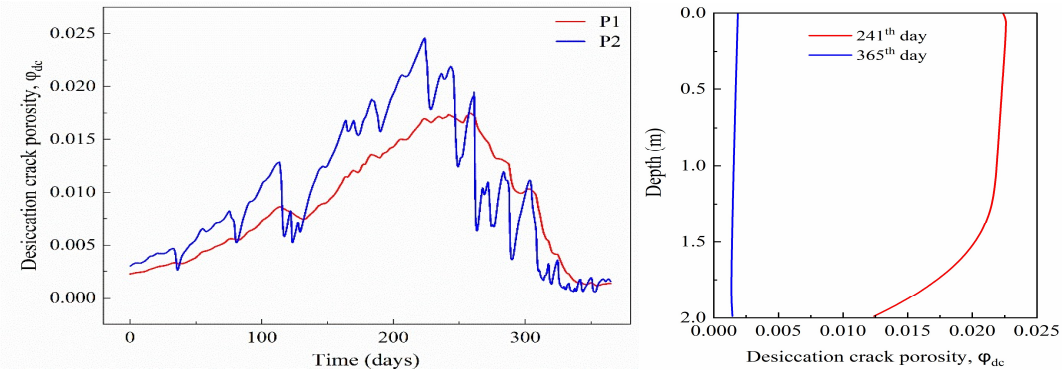

Figure 5: a) Desiccation crack porosity variation with time and b) Desiccation crack porosity with depth along A-A section

The spatial variation of φ_{dc} long the depth (A-A plane) is presented in Fig. 5b. The results reveal that crack opening and closure are not uniform across the depth. For instance, at the end of the

dry season, the crack porosity near the base of the surficial layer is significantly lower compared to the top, highlighting the non-uniform nature of desiccation cracking across the soil profile.

Effective saturation profile

Fig. 6a and 6b compare the effective saturation (S_e) profiles along the A-A plane for models without and with a desiccation crack layer, respectively. In the model without a desiccation crack layer, as shown in Fig. 6a, the low saturated hydraulic conductivity of the matrix domain restricts moisture movement within the subgrade. Consequently, no significant variation in effective saturation is observed across the seasons, with the subgrade remaining relatively stable in its moisture distribution. Conversely, in the model with a desiccation crack layer, the preferential flow of water through the cracks induces substantial variation in the S_e profile (Fig. 6b). At the pavement surface, effective saturation decreases drastically from 0.92 to 0.66 during the dry season, reflecting substantial moisture loss. Following the onset of rainfall in the wet season, S_e recovers, reaching 0.93 by the end of the simulation. This demonstrates a complete dry-wet cycle, despite the absence of direct moisture exchange between the pavement surface and the subgrade. Moreover, the effects of desiccation cracks are not confined to the top 2 m of the cracked surficial layer. The results show that moisture variation extends at least 1 m below this layer. This highlights the role of desiccation cracks in accelerating moisture movement into the stable subgrade layers beneath, emphasizing the interconnected impact of cracks on subsurface hydrology.

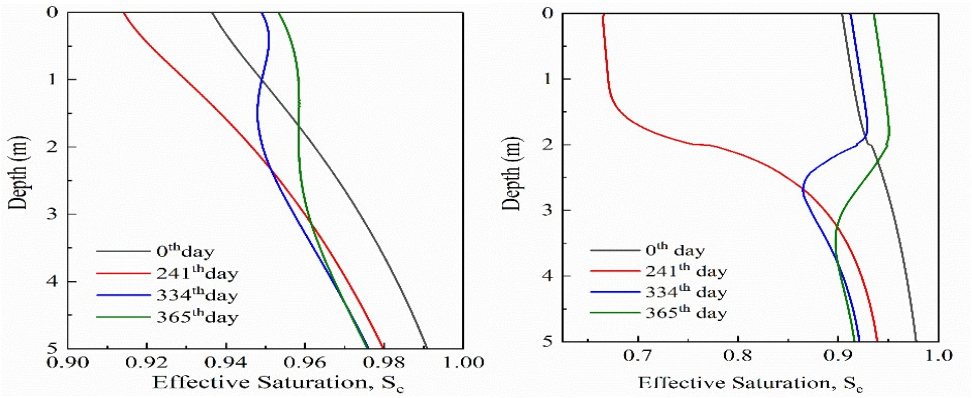

Figure 6: Effective saturation profile at section A-A of the model a) without crack layer and b) with crack layer

Heave and Settlement

The vertical deformation was calculated using Eq. 5 and is presented in Fig. 7a and 7b for models without and with a surficial crack layer, respectively along B-B plane. In the absence of desiccation cracks, the subgrade exhibits minimal deformation. A maximum settlement of 6 mm occurs during the dry season, followed by a heave of 8 mm in the wet season. This indicates a relatively stable subgrade with only minor seasonal variations in vertical deformation. In contrast, the presence of desiccation cracks leads to substantial deformation in the subgrade. The dry season results in a maximum settlement of 35 mm—nearly six times greater than that

observed in the model without cracks. During the wet season, significant heaving occurs, with a maximum value of approximately 30 mm.

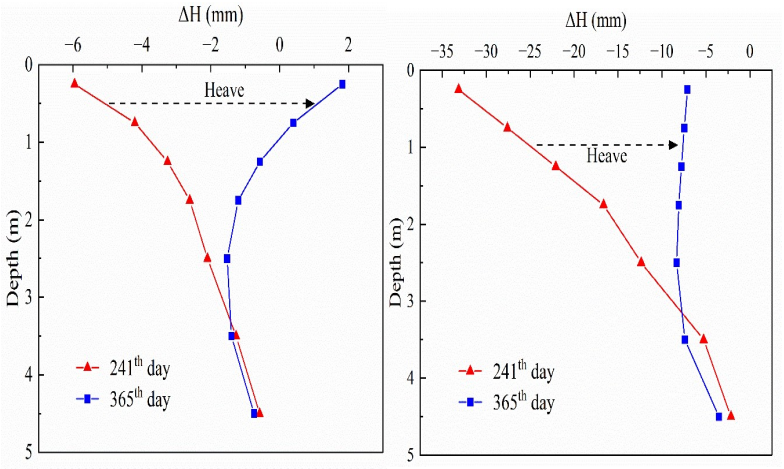

Figure 7: Vertical deformation profile at section B-B for the model a) without crack layer and b) with crack layer

Conclusion

This research utilized a numerical modelling approach to analyze the deformation behaviour of low-volume flexible pavements resting on expansive subgrade soils. The study investigated the impact of desiccation cracks and preferential flow on the heave and settlement behaviour of subgrade soils, offering critical insights into the interaction between hydraulic processes and deformation in cracked expansive subgrade.

The dynamics of crack volume revealed that desiccation cracks exhibit significant seasonal variation. During the dry season, moisture loss results in an increase in crack porosity, while the wet season reduces it, leading to partial or complete crack closure. This depth-dependent variation indicates that the crack network provides preferential pathways for moisture movement, even in regions where direct evaporation is restricted.

The influence of desiccation cracks on vertical deformation was evident in the comparison between models with and without cracks. Without cracks, the subgrade exhibited minimal settlement and heave, whereas the cracked model showed higher settlement and significant heave during wetting.

References

[1] K. Gaspard, Z. Zhang, G. Gautreau, M. Abufarsakh, and M. Martinez. Impact of Inundation on Roadway Pavements: Case Study – LA 493. Baton Rouge, LA: Louisiana Transportation Research Center, 2019.

[2] C. B. R. Christopher, C. Schwartz, and R. Boudreau. Geotechnical aspects of pavements. FHWA NHI-05-037, Federal Highway Administration, US DOT, Washington, D.C., 2006.

[3] M. S. M. Ghavami, M. S. Hosseini, P. D. Zavattieri, and J. E. Haddock. Flexible pavement drainage system effectiveness. *Construction and Building Materials*, 218:99–107, 2019. https://doi.org/10.1016/j.conbuildmat.2019.05.088.

[4] G. H. Roodi and J. G. Zornberg. Long-term field evaluation of a geosynthetic-stabilized roadway founded on expansive clays. *Journal of Geotechnical and Geoenvironmental Engineering*, 146(4):05020001, 2020.

[5] A. Askar and Y. C. Jin. Macroporous drainage of unsaturated swelling soil. *Water Resources Research*, 36(5):1189–1197, 2000: https://doi.org/10.1029/2000WR900023

[6] A. Coppola, A. Comegna, G. Dragonetti, H. H. Gerke, and A. Basile. Simulated preferential water flow and solute transport in shrinking soils. *Vadose Zone Journal*, **14**(9):1–22, 2015. https://doi.org/10.2136/vzj2015.02.0021.

[7] W. Shao, Z. Yang, J. Ni, et al. Comparison of single- and dual-permeability models in simulating the unsaturated hydro-mechanical behavior in a rainfall-triggered landslide. *Landslides*, 15:2449–2464, 2018. https://doi.org/10.1007/s10346-018-1059-0

[8] H. H. Gerke and M. T. Van Genuchten. A dual-porosity model for simulating the preferential movement of water and solutes in structured porous media. *Water Resources Research*, 29:305–319, 1993. https://doi.org/10.1029/92wr02339.

[9] M. T. Van Genuchten. A closed-form equation for predicting the hydraulic conductivity of unsaturated soils. *Soil Science Society of America Journal*, 44:892–898, 1980. https://doi.org/10.2136/sssaj1980.03615995004400050002x.

[10] R. D. Stewart, D. E. Rupp, M. R. A. Najm, and J. S. Selker. A unified model for soil shrinkage, subsidence, and cracking. *Vadose Zone Journal*, 15:1–15, 2016a. https://doi.org/10.2136/vzj2015.11.0146.

[11] R. D. Stewart, M. R. Abou Najm, D. E. Rupp, and J. S. Selker. Modeling multidomain hydraulic properties of shrink-swell soils. Water Resources Research, 52:7911–7930, 2016b. https://doi.org/10.1002/2016WR019336

[12] B. T. Brake, M. J. Van Der Ploeg, and G. H. De Rooij. Water storage change estimation from in situ shrinkage measurements of clay soils. *Hydrology and Earth System Sciences*, 17:1933–1949, 2013. https://doi.org/10.5194/hess-17-1933-2013.

[13] Y. Luo, J. Zhang, Z. Zhou, J. P. Aguilar-Lopez, R. Greco, and T. Bogaard. Effects of dynamic changes of desiccation cracks on preferential flow: experimental investigation and numerical modeling. *Hydrology and Earth System Sciences*, 27:783–808, 2023. https://doi.org/10.5194/hess-27-783-2023.

[14] *IS 2720 (Part 40): Method of Test for Soils – Determination of Free Swell Index of Soils*. Bureau of Indian Standards, New Delhi, India, 1977.

[15] S. Roy and S. Rajesh. Simplified model to predict features of soil–water retention curve accounting for stress state conditions. *International Journal of Geomechanics*, 20(3):04019191, 2020. https://doi.org/10.1061/(ASCE)GM.1943-5622.0001591.

[16] C. M. Jadar and S. Rajesh. Efficacy of utilizing Stress-Dependent SWRC in the analysis of a footing resting on an unsaturated soil slope. *International Journal of Geomechanics*, 24, 2024. https://doi.org/10.1061/ijgnai.gmeng-10340.